RESEARCH PAPER

Methylene blue inhibits function of the 5-HT transporter

Murat Oz[1,4], Dmytro Isaev[1], Dietrich E Lorke[2,3], Muhammed Hasan[1], Georg Petroianu[3] and Toni S Shippenberg[4]

[1]*Functional Lipidomics Branch, Department of Pharmacology,* [2]*Department of Anatomy, Faculty of Medicine and Health Sciences, UAE University, Al Ain, UAE,* [3]*Department of Cellular Biology & Pharmacology, College of Medicine, Florida International University, Miami, FL, USA, and* [4]*Integrative Neuroscience Section, Intramural Research Program, National Institute on Drug Abuse, National Institutes of Health, U.S. Department of Health and Human Services, Baltimore MD, USA*

BACKGROUND AND PURPOSE

Methylene blue (MB) is commonly employed as a treatment for methaemoglobinaemia, malaria and vasoplegic shock. An increasing number of studies indicate that MB can cause 5-HT toxicity when administered with a 5-HT reuptake inhibitor. MB is a potent inhibitor of monoamine oxidases, but other targets that may contribute to MB toxicity have not been identified. Given the role of the 5-HT transporter (SERT) in the regulation of extracellular 5-HT concentrations, the present study aimed to characterize the effect of MB on SERT.

EXPERIMENTAL APPROACH

Live cell imaging, in conjunction with the fluorescent SERT substrate 4-(4-(dimethylamino)-styryl)-*N*-methylpyridinium (ASP[+]), [3H]5-HT uptake and whole-cell patch-clamp techniques were employed to examine the effects of MB on SERT function.

KEY RESULTS

In EM4 cells expressing GFP-tagged human SERT (hSERT), MB concentration-dependently inhibited ASP[+] accumulation (IC$_{50}$: $1.4 \pm 0.3 \mu M$). A similar effect was observed in N2A cells. Uptake of [3H]5-HT was decreased by MB pretreatment. Furthermore, patch-clamp studies in hSERT expressing cells indicated that MB significantly inhibited 5-HT-evoked ion currents. Pretreatment with 8-Br-cGMP did not alter the inhibitory effect of MB on hSERT activity, and intracellular Ca^{2+} levels remained unchanged during MB application. Further experiments revealed that ASP[+] binding to cell surface hSERT was reduced after MB treatment. In whole-cell radioligand experiments, exposure to MB ($10 \mu M$; 10 min) did not alter surface binding of the SERT ligand [125I]RTI-55.

CONCLUSIONS AND IMPLICATIONS

MB modulated SERT function and suggested that SERT may be an additional target upon which MB acts to produce 5-HT toxicity.

Abbreviations

AFU, arbitrary fluorescent unit; ASP[+], 4-(4-(dimethylamino)-styryl)-*N*-methylpyridinium); GFP, green fluorescent protein; hSERT, human 5-HT transporter; KR, Krebs–Ringer

Introduction

Methylene blue (MB), a phenothiazine cationic dye, is used therapeutically to treat a range of conditions, including methaemoglobinaemia, malaria and vasoplegic shock (see, Wainwright and Crossley, 2002; Oz *et al.*, 2009). In addition,

it is used preoperatively to visualize various tissues (e.g. parathyroid glands and lymphatic nodes during surgery) (Dudley, 1971; Muslumanoglu *et al.*, 1995; Kuriloff and Sanborn, 2004). However, an increasing number of studies have documented that, in patients taking serotonin reuptake inhibitors (SRIs), such as duloxetine, sibutramine,
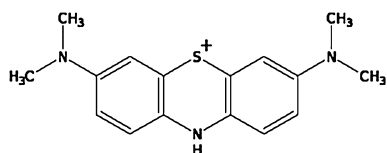
Figure 1

Chemical structure of MB.

venlafaxine, clomipramine and imipramine, intravenous infusion of MB can precipitate 5-HT toxicity or a 5-HT syndrome, characterized by prolonged disorientation, dizziness, headache, tremors, seizures and mental confusion during the postoperative period (Bach *et al.*, 2004; Gillman, 2006; 2008; 2011; Kartha *et al.*, 2006; Ng and Cameron, 2010). For this reason, the clinical use of MB in patients taking monoamine oxidase (MAO) inhibitors or 5-HT uptake blockers is contraindicated.

Metabolism of 5-HT by MAO-A and its reuptake by the 5-HT transporter (SERT) are the primary mechanisms that regulate extracellular 5-HT concentrations in the CNS. MAO-A inhibition has been suggested to play a role in mediating the toxic effects of MB in patients taking SRIs (Ramsay *et al.*, 2007). Although SERT is an integral membrane protein that plays a key role in regulating synaptic reuptake mechanism by clearing 5-HT released into the extracellular space (Amara and Kuhar, 1993), thereby regulating extracellular 5-HT concentrations, the effects of MB on SERT function are not known.

Recent studies have demonstrated that the use of the fluorescent monoamine transporter substrate ASP^+, 4-(4-(dimethylamino)-styryl)-*N*-methylpyridinium, in combination with confocal microscopy enables real-time, spatially resolved functional analysis of various monoamine transporters in heterologous expression systems and neuronal cultures (Schwartz *et al.*, 2003; 2006; Zapata *et al.*, 2007; Oz *et al.*, 2010a). Analysis of ASP^+ accumulation not only permits resolution of substrate binding and uptake by the same cell but also enables quantification of rapid (e.g. ≤ 1 min) changes in SERT function (Oz *et al.*, 2010b). In the present study, we have used live cell imaging of ASP^+ accumulation, patch-clamp techniques and whole-cell radioligand binding methods in heterologous expression systems to investigate the effect of MB (Figure 1) on SERT function.

Methods

Cell culture

Experiments were conducted in EM4 cells, a HEK-293 cell line that stably expresses a macrophage scavenger receptor to increase their adherence to tissue culture plastic (EM4 cells, R.A. Horlick, Pharmacopeia, Cranberry, NJ) and in Neuro2A (N2A) cells (American Type Culture Collection). EM4 and N2A cells were maintained in DMEM/F12 and MEM medium (cellgro®, Mediatech, Inc, Herndon, VA), respectively, and supplemented with 10 % fetal bovine serum (FBS, Invitrogen). They were grown in a humidified atmosphere at 37°C

and 5% CO_2. Twenty-four hours after plating, cells were transiently transfected using LTX (Invitrogen, Carlsbad, CA) according to the manufacturer's instructions. Experiments were performed 48 h after transfection when cells were 70% to 80% confluent.

ASP^+ uptake

For ASP^+ experiments, cells were seeded on day 1 at 1.4×10^5 cells per 35 mm Delta T Petri dish (Bioptechs, Butler, PA). Between 30 and 50 cells were used for each experiment unless otherwise stated. These cells were pooled from at least three separate transfections, with a minimum of two dishes analysed per transfection. Cells were transiently transfected with green fluorescent protein-tagged human SERT (GFP-hSERT). Previous studies have shown that addition of this tag does not alter SERT function (Schmid *et al.*, 2001). Immediately before experiments, growth media was removed, and cells were washed two times in Krebs–Ringer solution (KR; 130 mM NaCl, 1.3 mM KCl, 2.2 mM $CaCl_2$, 1.2 mM $MgSO_4$, 1.2 mM KH_2PO_4, 10 mM HEPES and 1.8 g·L^{-1} glucose, pH 7.4) buffer. After washing, fresh KR solution was added to the culture dish, which was then mounted on the stage of a Zeiss LSM 510 microscope confocal system. Time-resolved quantification of SERT function in single cells was achieved using the fluorescent SERT substrate ASP^+. A within-cell design was used to assess the effects of MB on ASP^+ uptake. The microscope was focused on the centre of a monolayer of cells, and background autofluorescence was determined by collecting an image immediately before replacement of the KR solution containing ASP^+ (10 μM). The rate (slope of the linear accumulation function) of ASP^+ uptake was then measured for 1 min immediately before drug addition. Vehicle or drug was added, and the slope of ASP^+ accumulation was again determined over a 10 min period. Control studies showed that ASP^+ uptake by SERT is linear for 10–15 min after ASP^+ addition. It is dependent on temperature and extracellular concentrations of Na^+, Cl^- and is inhibited by SERT substrates (Oz *et al.*, 2010b). Images were collected every 20 s to enable capture of ASP^+ fluorescence (excitation, 488 nm; emission, 607–652 nm). The influence of drug pretreatment on ASP^+ uptake was assessed by comparing the slope values during control conditions (determined 1 min before the addition of test compounds) with those acquired 10 min after addition of vehicle (distilled water) or test compound.

Image analysis

ASP^+ fluorescence accumulation was determined from the average pixel intensity at each time point accumulated within the cell using NIH-image-J, the boundaries of which were determined from a reference picture at the initial time point of GFP fluorescence (indicating the presence of GFP-hSERT at the plasma membrane). Values are expressed as the percentage change in ASP^+ accumulation rate after the addition of drug.

[^{3}H]Alanine uptake

EM4 cells (plated at 10^{-5} cells per well) were transfected with hSERT as described above. Uptake assays were conducted as described previously with minor modification (Zapata *et al.*, 2007). Briefly, the medium was removed by aspiration, and

cells were washed twice with 1.0 mL of KR buffer, pH 7.4. Cells were then pre-incubated with MB (10 µM) for 10 min. Uptake was initiated by addition of 100 nM [³H]alanine (82 Ci·mmol⁻¹, PerkinElmer, Boston, MA). After 5 min, uptake was terminated by aspiration of the incubation solution and rapidly washing (3× with cold KR assay buffer). Cells were lysed in 0.1% SDS, and accumulated radioactivity was measured (triplicates of 100 µL aliquots of lysed cell preparation) by liquid scintillation counting. For each experiment, non-specific [³H]alanine uptake was defined in parallel experiments as the alanine accumulation in the presence of sodium-free buffer and was subtracted from total counts. Sodium-free buffer was prepared by replacing NaCl with an equimolar concentration of *N*-methyl-*D*-glucamine chloride. The pH was adjusted to 7.4 with KOH. Protein concentrations of lysed cell preparations were determined using a protein assay kit (Bradford assay, Bio-Rad, Richmond, CA).

Ca²⁺ imaging

Fluo-3-AM (Invitrogen) was used to monitor changes in intracellular Ca^{2+} levels. Cells were washed twice with 1 mL of KR solution and incubated in 10 µM Fluo 3-AM for 45 min in 37°C. Following pretreatment, cells were washed three times in 1 mL KR solution and placed on the stage of a Zeiss LSM 510 microscope. Analysis of fluorescent intensity was performed using Image J software and presented as arbitrary fluorescent units (AFU). Background fluorescence were subtracted, and the intensity levels were determined before (controls) and during the treatment conditions for each cell. Fluo-3-AM and A23187 were dissolved in DMSO and kept as stock solutions (10 mM) at −20°C.

[³H]5-HT uptake

One day after transfection, cells were assayed for [³H]5-HT transport as described previously (Ramamoorthy *et al.*, 1998). Briefly, cells were washed in assay buffer (130 mM NaCl, 1.3 mM KCl, 2.2 mM CaCl₂, 1.2 mM MgSO₄, 1.2 mM KH₂PO₄ and 10 mM HEPES, pH 7.4), followed by incubation in 37°C assay buffer containing 1.8 g·L⁻¹ glucose, 100 µM pargyline and 100 µM ascorbic acid for 10 min with or without agonist. 5-HT uptake was initiated by the addition of [³H]5-HT (20 nM final concentration). The reaction (10 min at 37°C) was terminated by washing three times with ice-cold assay buffer. The cells were dissolved in OptiPhase scintillation fluid (PerkinElmer, Gaithersburg, MD), and [³H]5-HT accumulation was determined by liquid scintillation. Specific 5-HT uptake was determined by subtracting the amount accumulated in the presence of 1 µM paroxetine. All transport assays were performed in triplicate, and the mean values for specific uptake ± SEM of eight separate experiments were determined.

Whole-cell radioligand binding assay

The level of surface membrane expression of the hSERT was determined using a whole-cell binding assay as described earlier (Zhu *et al.*, 2004). The transfected EM4 cells were grown for 48 h in a 96-well plate, and washed twice with ice-cold phosphate-buffered saline containing 0.1 mM CaCl₂ and 1 mM MgCl₂, pH 7.2 (PBSCM) before incubation. The 96-well plate was placed on ice, and the cells were pre-incubated 5 min with PBSCM or PBSCM containing 10 µM paroxetine or 200 µM 5-HT. PBSCM containing [¹²⁵I]RTI-55 was added to a final concentration of 20 nM in the absence and presence of 10 µM MB. After 30 min incubation, the cells were washed twice with ice-cold PBSCM. Subsequently, 50 µL of scintillation solution (Microscint 20; PerkinElmer Life Sciences, Boston, MA) was added to each well. Bound radioactivity was determined by direct counting of plates using a PerkinElmer microplate scintillation counter. [¹²⁵I]RTI-55 and paroxetine are membrane permeable and pre-incubation with 10 µM paroxetine blocks the total whole cell [¹²⁵I]RTI-55 binding sites. 5-HT is not membrane permeable at 4°C, and pre-incubation thus blocks all external [¹²⁵I]RTI-55 binding sites. The non-specific binding was determined by measuring the amount of [¹²⁵I]RTI-55 bound after pre-incubation with paroxetine. Surface expression levels were calculated as the fraction of [¹²⁵I]RTI-55 binding sites that were blocked by 100 µM 5-HT.

Electrophysiological experiments

The external (bathing) solution has been described above (KR buffer). Patch pipettes were filled with 120 mM KCl, 10 mM HEPES, 1.1 mM EGTA, 0.1 mM CaCl₂, 2 mM MgCl₂ and 30 mM dextrose, adjusted to pH 7.35 with KOH. Patch electrodes were pulled from borosilicate glass capillaries with a programmable Flaming-Brown micropipette puller (P-97; Sutter Instruments Co., Novato, CA) and heat-polished to a final tip resistance of 2–4 MΩ. Whole cell currents were recorded at room temperature (22°C), using an Axopatch 200B amplifier and the PClamp 8.1 software (Axon Instruments, Foster City, CA). Currents were low-pass filtered at 1 kHz, stored on an IBM compatible computer and analysed off-line by the Clampfit programme (Axon Instruments). Drugs were applied by gravity perfusion. Cells were continuously superfused with bathing solution in the absence and presence of applied drugs. The cells were voltage-clamped at a holding potential of −60 mV. Alternatively, substances were examined using voltage steps from −60 mV to potentials between −120 and 0 mV. Net currents were displayed as 5-HT-induced inward currents minus background (control) currents.

Data analyis

Data are expressed as mean ± standard error of means (SEM). Statistical significance at the level of 0.05 was determined by Student's *t*-test or one-way ANOVA using the computer software Origin™ (Originlab Corp. Northampton, MA). Fluorescent images were processed using Image J software (W. Rasband, NIH).

Materials

MB, A23187, ASP⁺ and 8-Br-cGMP were obtained from Sigma-RBI (St. Louis, MO). BAPTA-AM was purchased from Calbiochem (San Diego, CA). [³H]-5-HT and [¹²⁵I]RTI-55 were obtained from Amersham Biosciences, Inc. (Piscataway, NJ) and PerkinElmer Life Sciences (Boston, MA) respectively.

Results

ASP⁺ rapidly accumulated in the cytoplasm of EM4 cells transfected with GFP-hSERT (Figure 2A) but not in untransfected
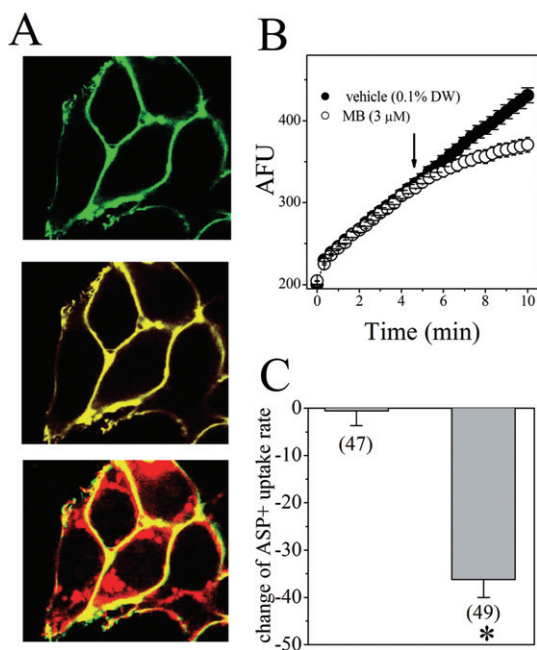
Figure 2

The effect of MB on ASP$^+$ uptake in EM4 cells transiently transfected with GFP-hSERT. Confocal images presented in panel A show an image of cells expressing GFP-hSERT. GFP-hSERT is indicated by green fluorescence and ASP$^+$ by red fluorescence. Co-localization of the two fluorophores is indicated by the merged images (yellow). GFP-hSERT and ASP$^+$ localization before time 0 (top panel) or 5 s (middle panel) and 40 s (lower panel) after ASP$^+$ addition are shown. These images show that ASP$^+$ rapidly binds to hSERT located on the cell surface followed by a slower phase of intracellular ASP$^+$ accumulation. (B) Time course of mean ASP$^+$ uptake in control and MB-treated cells (n = 8–9 cells per treatment) is shown. Note the initial rapid binding phase after ASP$^+$ addition followed by the linear uptake phase. Addition of MB (3 µM) decreases the rate of ASP$^+$ uptake relative to vehicle (distilled water) values. The change in hSERT function is presented as the change in the slope of uptake measured for 1 min immediately before and 5 min after MB addition. Each data point represents the mean ± SEM fluorescent intensity, which was calculated as AFU. (C) The bar graph compares the changes in ASP$^+$ accumulation rates calculated after 5 min application of vehicle (0.1% distilled water) or MB. The data are from three different experiments. The numbers of cells are presented below each bar. *P < 0.01, significantly different.

Figure 3

MB inhibits ASP$^+$ accumulation in a time- and concentration-dependent manner in EM4 cells and in N2A neuronal cells. (A) Time course of the effect of MB on ASP$^+$ accumulation in EM4 cells. Each data point represents the means ± SEM of eight to nine cells. *P < 0.01, significantly different. from control measurements, taken before the addition of MB. (B) Concentration-dependent effect of MB on ASP$^+$ accumulation in EM4 cells. Each concentration of MB was applied for 5 min, and changes in ASP$^+$ uptake rates were plotted. Data points represent the mean ± SEM of three different experiments (n = 50–67). (C) MB inhibits ASP$^+$ accumulation in N2A neuronal cell lines in a concentration-dependent manner. Results are expressed as the mean ± SEM. Data are from three separate experiments, and in each experiment, at least two different dishes were analysed (n = 27–39).

cells. Consistent with a recent study (Oz *et al.*, 2010a), two distinct phases of ASP$^+$ incorporation were observed (Figure 1A and B). Rapid (<1 s) initial binding of ASP$^+$ to hSERT located on the cell surface was followed by a slower (seconds-minutes) phase of cytoplasmic accumulation of ASP$^+$ signal. The effect of MB on the function of hSERT was determined by measuring the rate of ASP$^+$ accumulation before and after the addition of 3 µM MB (Figure 2B). Application of 3 µM MB for 10 min significantly decreased the rate of ASP$^+$ accumulation (Figure 2C: Student's *t*-test, $P \le 0.001$).

The inhibition of ASP$^+$ accumulation was apparent within 1 min after MB addition and reached equilibrium within 10 min. (Figure 3A). Fifty percent inhibition ($\tau_{1/2}$) was reached 3.1 ± 0.4 min (mean ± SEM) after MB addition. Analysis of

the slope of ASP$^+$ accumulation in response to graded concentrations of MB (Figure 3B) revealed an IC$_{50}$ value of 1.2 ± 0.3 µM and a slope value of 1.4. To determine whether MB modulation of hSERT occurs in neuronal cell lines, ASP$^+$ uptake was examined in N2A cells transiently transfected with GFP-hSERT. As observed with EM4 cells, 10 min application of MB (1–10 µM) to N2A cells expressing hSERT significantly decreased ASP$^+$ uptake in a concentration-dependent manner (Figure 3C; Student's *t*-test: t = –9.5; d.f. = 51; $P \le 0.001$).

MB is commonly used to inhibit soluble guanylate cyclase (Mayer *et al.*, 1993; Moncada and Higgs, 2006). Since changes in intracellular cGMP and Ca^{2+} levels regulate SERT function (Miller and Hoffman, 1994; Zhu *et al.*, 2004; 2007), inhibition
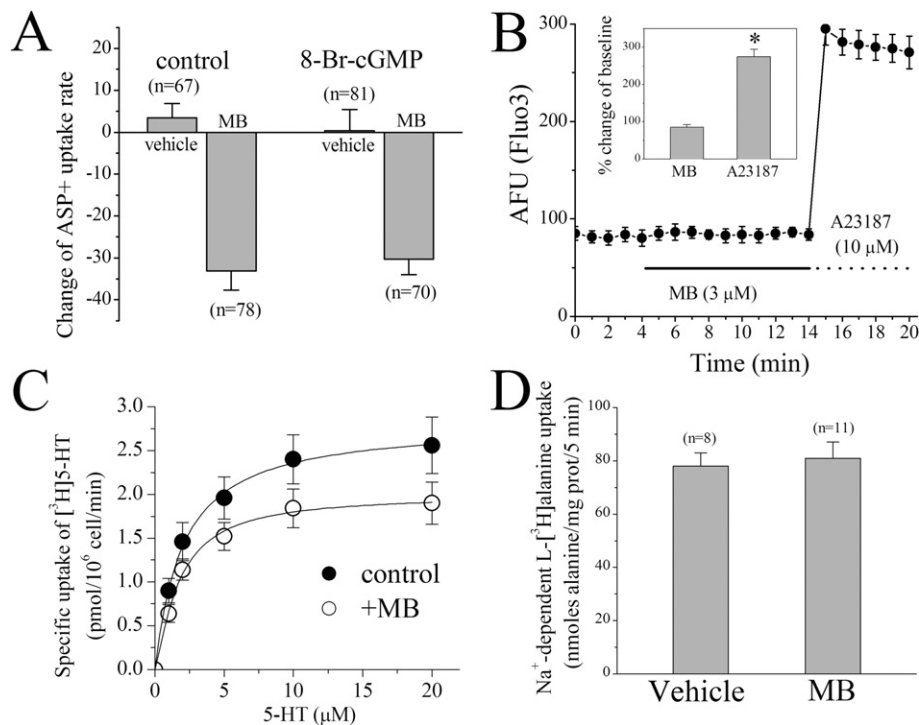
Figure 4

The effects of MB on [³H]5-HT uptake, [³H]alanine uptake and intracellular Ca^{2+} levels and the influence of cGMP on MB inhibition of hSERT function. (A) The effects of 5 min application of 3 µM MB with vehicle or pretreatment with 8-Br.cGMP (10 min; 100 µM). Data points represent the mean ± SEM of three different experiments. The numbers of cells are presented above each data point. (B) The effect of 5 min application of 3 µM MB on intracellular Ca^{2+} levels in Fluo3-AM (10 µM) loaded cells. Data points indicate the mean ± SEM fluorescent intensity (AFU) from 11 cells. *Inset* shows percent changes in the presence of MB (5 min, 3 µM) or A23187 (5 min, 10 µM) compared with baseline values at 4 min. *$P < 0.01$, significantly different. (C) EM4 cells stably expressing hSERT (10^5 cells per well) were incubated in a final volume of 0.1 mL containing the indicated concentrations of [³H]5-HT in the absence or presence of 3 µM MB for 1 min at 22°C. Non-specific uptake (measured in the presence of 1 µM paroxetine) was less than 10% and was subtracted. The symbols represent mean ± SEM of three experiments carried out in triplicate. (D) The effects of 10 min application of 10 µM MB on Na^+-dependent [³H]alanine uptake. Data points represent the mean ± SEM of three different experiments. The numbers of cells are presented above each data point.

of guanylate cyclase activity by MB could mediate its effects on SERT function (Figure 4A). To test this hypothesis, ASP^+ uptake was quantified in EM4 cells pre-incubated for 30 min with 8-Br-cGMP (100 µM), a membrane permeable analogue of cGMP. Incubation of cells with 8-Br-cGMP alone did not alter ASP^+ uptake. The magnitude of MB-induced SERT inhibition did not differ in control or 8-Br-cGMP-treated cells (ANOVA, $F_{1,292} = 0.12$; $P = 0.74$). Next, we investigated the influence of MB on intracellular Ca^{2+} levels in EM4 cells pre-loaded with the membrane permeable Ca^{2+} indicator Fluo3-AM (10 µM for 30 min) before MB (10 µM) addition. Application of MB for 10 min did not alter basal fluorescent intensity (Figure 4B; Student's *t*-test: $P = 0.553$). In contrast, exposure of cells to the 10 µM Ca^{2+} ionophore, A23187 (Case *et al.*, 1974), for 5 min significantly increased intracellular Ca^{2+} levels (*inset* to Figure 4B; Student's *t*-test: $P \leq 0.001$).

In addition to ASP^+, we investigated the ability of MB to modulate the uptake of [³H] 5-HT in hSERT-expressing EM4 cells (Figure 4C). Pre-incubation of cells with 10 µM MB for 10 min caused a significant reduction in [³H]5-HT uptake (Student's *t*-test: $P \leq 0.001$). To assess whether the reduced SERT activity in response to MB was due to an alteration of Na^+ electrochemical gradients across membranes or the lipid

bilayer structure, we examined the effect of MB on Na^+-dependent transport of alanine. Ten-minute incubation with 10 µM MB did not alter [³H]alanine uptake in SERT-transfected EM4 cells (Figures 4D and 95.6 ± 2.4% of controls; ANOVA, $F_{1,18} = 4.1$; $P = 0.059$; $n = 10$).

We also investigated the effect of MB on hSERT-mediated ion currents using a whole-cell patch-clamp technique. In EM4 cells transfected with hSERT and clamped at a holding potential of –60 mV, bath application of 30 µM 5-HT induced an inwardly directed current. Co-application of 5-HT and the uptake blocker citalopram (1 µM) completely blocked the 5-HT-evoked current (shown in Figure 5A). 5-HT-activated currents measured at test potential of –120 mV were significantly decreased after 10 min application of 3 µM MB (Student's *t*-test; $P \leq 0.001$). In the voltage range of –120 to 0 mV, magnitudes of net currents induced by 5-HT applications were decreased after 10 min application of 3 µM MB (Figure 5B and C).

Changes in 5-HT uptake could involve alterations in transporter surface trafficking, a decrease of catalytic function, or both. To establish whether the inhibition of the 5-HT binding phase observed after 10 min MB (3 µM) pre-incubation is paralleled by changes in cell surface SERT, we

A

1 μM citalopram
control
3 μM MB
30 μM 5-HT

50 pA

100 ms

B

● 5-HT
○ +MB
▲ control
△ citalopram

Voltage (mV)

Current (pA)

C

Voltage (mV)

Net 5-HT current (pA)

● 5-HT
○ +MB
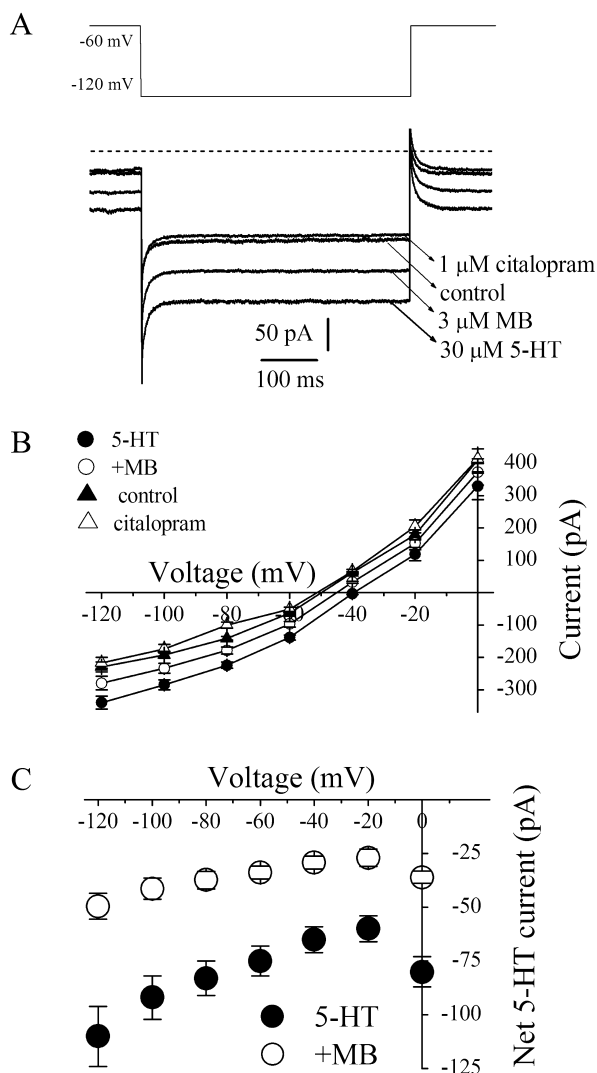
Figure 5

MB inhibits the hSERT mediated 5-HT induced currents in EM4 cells. (A) 5-HT (30 μM)-induced whole-cell currents recorded in EM4 cells in the absence and presence of citalopram (1 μM) or MB (3 μM). (B) Steady-state current–voltage (*I–V*) curves for 5-HT-induced currents in hSERT-transfected EM4 cells. Citalopram (1 μM) was added to 5-HT to test for inhibitor sensitivity. Symbols represent the means ± SEM of five experiments. The background *I–V* curves were obtained under control conditions (no 5-HT, no inhibitor). The steps to the test voltages from the holding potential of –60 mV lasted 500 ms. Steady-state current was defined as the average current during 400–500 ms The membrane potential was held at –60 mV, and then the voltage was stepped to a potential between –120 and 0 mV in 20 mV increments. (C) Subtracted cumulative data for net 5-HT-induced steady-state currents. The difference currents in controls (5-HT-CON) and after MB (3 μM; 10 min) treatment (MB-CON) illustrated in Figure 4A are plotted against the test voltage. Values are means ± SEM, *n* = 5.

implemented a previously described whole-cell radioligand binding technique using [^{125}I]RTI-55, a membrane-permeable cocaine analogue that labels both surface and intracellular sites (Zhu *et al.*, 2004). We used either paroxetine (10 μM) as
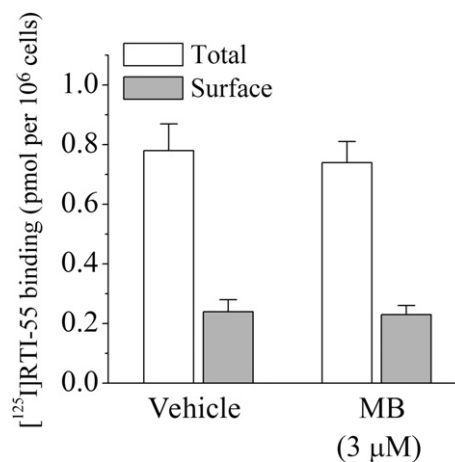
Figure 6

The effects of MB on the surface expression of SERT in EM4 cells. EM4 cells were transfected with hSERT and assayed for the fraction of hSERT expressed at the plasma membrane in the absence and presence of 10 μM MB. Total specific binding as defined by subtracting the binding of [^{125}I]RTI-55 (20 nM) achieved in the presence of paroxetine (10 μM) alone from total binding and surface-specific binding as calculated by subtracting [^{125}I]RTI-55 binding in the presence of 100 μM 5-HT from that of [^{125}I]RTI-55 alone. Data are given as mean ± SEM from three separate experiments (*n* = 11–14). No significant difference between MB and the vehicle was detected.

displacer to monitor total (surface plus intracellular) specific binding or the hydrophilic ligand 5-HT (100 μM) as displacer to define surface binding. Our assay temperature (4°C) was chosen to limit 5-HT uptake as well as transporter exocytosis/endocytosis. Results of [^{125}I]RTI-55 binding experiments indicated that total and surface hSERT bindings were not significantly altered in the presence of MB (Figure 6).

Discussion

The present studies used *in vitro* assays to examine the influence of acute MB exposure on SERT function. MB exposure significantly decreased ASP$^+$ accumulation, [^{3}H]5-HT uptake and 5-HT-evoked currents in EM4 cells expressing hSERT. Decreased ASP$^+$ accumulation was also observed in the N2A cell line. The down-regulation of function produced by MB was insensitive to cGMP inhibition and was not associated with alterations in intracellular Ca^{2+} concentrations. Cell surface binding of [^{125}I]RTI-55 was unchanged following MB treatment. However, [^{125}I]RTI-55 binds to both functional and non-functional SERT expressed on the cell surface. Therefore, [^{125}I]RTI-55 binding studies do not allow the assessment of SERT function.

Previous studies have demonstrated the utility of the ASP$^+$ imaging technique for quantifying real-time changes in monoamine transporter function (Schwartz *et al.*, 2003; Zapata *et al.*, 2007; Oz *et al.*, 2010a). We have recently shown that intracellular accumulation of ASP$^+$, a fluorescent substrate for SERT (Oz *et al.*, 2010b), is saturable, temperature-dependent and decreased by transporter substrates and

inhibitors. In contrast, manipulations that increase SERT function increase uptake. Fast acquisition of confocal images allowed us to examine the kinetics of ASP$^+$ binding. We have employed this method in our earlier studies on dopamine (Oz et al., 2010a) and 5-HT (Oz et al., 2010b) transporters. This technique is employed to measure changes in the maximal number of binding sites of SERT expressed on the cell surface. In our [^{125}I]RTI-55 studies, however, the number of these binding sites was not altered by MB. Together these findings demonstrate that changes in ASP$^+$ accumulation reflect a transporter-mediated process. Furthermore, as ASP$^+$ accumulation is linear for at least 10 min after its addition, a within-cell design can be used to monitor time-related alterations in SERT function in living cells. Exposure of EM4 cells to MB produced a rapid and concentration-dependent decrease in ASP$^+$ accumulation. Decreased accumulation was also observed in N2A cells transfected with hSERT. These data indicate that acute MB exposure down-regulates SERT function. Furthermore, time course studies show that down-regulation persists for at least 10 min after MB addition.

Radioligand uptake studies and patch clamp recordings provide additional evidence that SERT function is down-regulated following MB exposure. Thus, 10 min incubation of cells with MB (3–10 µM) reduced [^{3}H]5HT uptake and 5-HT-induced ion currents, indicating that endogenous ligand uptake was also affected by MB. Importantly Na$^+$-dependent alanine uptake was not affected by an MB concentration that significantly decreased ASP$^+$ accumulation and [^{3}H]5HT uptake. Thus, the functional interaction of MB with SERT cannot be attributed to alterations in Na$^+$ electrochemical gradient or to non-specific perturbations of the lipid bilayer.

In patch-clamp studies, as previously reported (Hilber et al., 2005), addition of 5-HT to the extracellular solution induced an inward current that was completely inhibited by co-administration of the selective 5-HT uptake inhibitor citalopram, indicating that 5-HT-induced currents are mediated by hSERT expressed in EM4 cells. In line with the ASP$^+$ uptake studies, pre-application of MB significantly reduced hSERT-mediated currents, further suggesting that MB down-regulates the function of hSERT.

MB inhibits soluble guanylate cyclase and inhibits nitric oxide synthesis (Mayer et al., 1993; Moncada and Higgs, 2006). Manipulations that increase cGMP levels and intracellular Ca^{2+} concentrations enhance 5HT uptake (Miller and Hoffman, 1994; Ramamoorthy et al., 1998; Zhu et al., 2004; 2007), suggesting that MB-evoked inhibition of cGMP or changes in Ca^{2+} may underlie the interaction of MB with SERT. Incubation of cells with 8-Br-cGMP (100 µ) for 10 min did not alter the decrease in ASP$^+$ accumulation produced by 3 µM MB. Furthermore, imaging studies using the Ca^{2+} indicator Fluo-3 revealed no change in intracellular Ca^{2+} levels following MB treatment. Together, these data indicate that the MB-evoked down-regulation of SERT function is independent of changes in cGMP pathway and intracellular Ca^{2+} levels. It is important to note that MB causes direct actions on the functions of several ion channels, receptors and enzymes (see Oz et al., 2009; Oz et al., 2011). Therefore, MB may regulate the function of hSERT directly.

Manipulations of the transport, binding and metabolism of 5-HT by drugs such as SRIs, MAO inhibitors, or tricyclic anti-depressants result in significant changes in 5-HT levels and lead to clinically desired effects in the treatment of depression. While MB shows antidepressant actions in clinical trials (Naylor et al., 1986; 1987) and in various behavioural animal studies (Eroglu and Caglayan, 1997; Volke et al., 2003), excessive levels of 5-HT can also lead to a potentially life-threatening condition described as 5-HT toxicity characterized by the side effects such as euphoria, hyperreflexia and myoclonus (for reviews, Boyer and Shannon, 2005; Isbister and Buckley, 2005). In recent studies, in addition to MAO inhibition, regulation of SERT activity was also implicated in the pathogenesis of 5-HT toxicity. For example, 5-hydroxy-L-tryptophan (5-HTP), the precursor of 5-HT, increased 5-HT in various brain areas examined, with approximately two- to fivefold increases in SERT$^{+/+}$ mice, and greater, 4.5- to 11.7-fold, increases in SERT$^{-/-}$ mice (Fox et al., 2008). Furthermore, changes in extracellular 5-HT concentrations were associated with 5-HT toxicity-like behavioural changes (Fox et al., 2008), suggesting a role of SERT in 5-HT toxicity.

Clinically, MB is administered in a bolus dose of 1–2 mg·kg^{-1} body weight over 10–20 min (Harvey, 1980). A mean plasma concentration of 5 µM MB was reported after intravenous injection of 1.4 mg·kg^{-1} MB (Aeschlimann et al., 1996). Peak plasma concentrations in human subjects following intravenous injection of 0.75 mg·kg^{-1} MB were 500–600 ng·mL^{-1} (1.6 µM) (Walter-Sack et al., 2009; Gillman, 2011). The IC$_{50}$ value for MB effects on SERT function was 1.4 µM, suggesting that doses of MB used therapeutically may result in brain concentrations sufficient to produce alterations in SERT activity. Indeed, MB crosses the blood–brain barrier, when administered intraduodenally and intravenously (Peter et al., 2000), and accumulates in presynaptic nerve endings after systemic administration (Muller, 1992). Moreover, in rodents, brain MB concentrations following intravenous (20 mg·kg^{-1}) or oral administration (200 mg·kg^{-1}) were shown to be more than 500-fold higher than plasma concentrations (O'Leary et al., 2010). However, it should be noted that whole blood measurements of MB may not accurately reflect its bio-phase concentration, because MB binds to albumin and is taken up by blood cells (Buchholz et al., 2008). Therefore, concentrations of free MB are considerably lower (Buchholz et al., 2008; Oz et al., 2009). Furthermore, the potency of MB in affecting MAO-A is significantly greater than for SERT: whereas the IC$_{50}$ value for SERT inhibition is c. 1.4 µM, that for MAO-A inhibition is one order of magnitude lower (Ramsay et al., 2007). In addition, 5-HT toxicity after MB administration has only been reported in patients taking SRI medication (Gillman, 2010; 2011). Together these findings suggest that although the pharmacological actions of MB primarily reflect MAO-A inhibition, SERT inhibition may, in fact, contribute to toxicity associated with high doses of MB.

At the concentration range used in this study (1–30 µM), MB was demonstrated to modulate directly the function of various ion channels and receptors (see Oz et al., 2009). For example, MB inhibits functions of voltage-dependent sodium and potassium channels, muscarinic receptors and various enzymes (Oz et al., 2009). The reduced leuco-form of MB has pharmacological actions, different from those of its oxidized form, on the functions of various ion channels and enzymes (see Oz et al., 2011). However, absorption spectrum analysis of the MB and leuco-MB peak ratios indicated that leuco-MB was less than 0.5% of the MB in our assay system

(unpublished results; $n = 2$ measurements). Therefore, it is unlikely that actions of MB we observed were due to its reduced leuco form.

MB is a phenothiazine compound. Although most of the phenothiazines are clinically important drugs, including antipsychotics, antihistamines and anticholinergic agents, their effects on the monoamine transporters are largely unknown. Given our results, the question arises as to whether other drugs of the phenothiazine class could affect transporter function. Studies addressing this issue are currently in progress. In conclusion, our results indicated that MB inhibited the function of human SERT at clinically relevant concentrations. It appears that the cGMP pathway, intracellular Ca^{2+} levels and changes in hSERT surface expression were not involved in mediating the effects of MB on hSERT activity.

Acknowledgements

Conflict of interest

The authors of this manuscript have no conflict of interest to declare.

References

Aeschlimann C, Cerny T, Kupfer A (1996). Inhibition of (mono)amine oxidase activity and prevention of ifosfamide encephalopathy by methylene blue. Drug Metab Dispos 24: 1336–1339.

Amara SG, Kuhar MJ (1993). Neurotransmitter transporters: recent progress. Annu Rev Neurosci 16: 73–93.

Bach KK, Lindsay FW, Berg LS, Howard RS (2004). Prolonged postoperative disorientation after methylene blue infusion during parathyroidectomy. Anesth Analg 99: 1573–1574.

Boyer EW, Shannon M (2005). The serotonin syndrome. N Engl J Med 352: 1112–1120.

Buchholz K, Schirmer RH, Eubel JK, Akoachere MB, Dandekar T, Becker K et al. (2008). Interactions of methylene blue with human disulfide reductases and their orthologues from Plasmodium falciparum. Antimicrob Agents Chemother 52: 183–191.

Case GD, Vanderkooi JM, Scarpa A (1974). Physical properties of biological membranes determined by the fluorescence of the calcium ionophore A23187. Arch Biochem Biophys 162: 174–185.

Dudley NE (1971). Methylene blue for rapid identification of the parathyroids. Br Med J 3: 680–681.

Eroglu L, Caglayan B (1997). Anxiolytic and antidepressant properties of methylene blue in animal models. Pharmacol Res 36: 381–385.

Fox MA, Jensen CL, French HT, Stein AR, Huang SJ, Tolliver TJ et al. (2008). Neurochemical, behavioral, and physiological effects of pharmacologically enhanced serotonin levels in serotonin transporter (SERT)-deficient mice. Psychopharmacology (Berl) 201: 203–218.

Gillman PK (2006). Methylene blue implicated in potentially fatal serotonin toxicity. Anaesthesia 61: 1013–1014.

Gillman PK (2008). Methylene blue is a potent monoamine oxidase inhibitor. Can J Anaesth 55: 311–312.

Gillman PK (2010). Methylene blue and serotonin toxicity: definite causal link. Psychosomatics 51: 448–449.

Gillman PK (2011). CNS toxicity involving methylene blue: the exemplar for understanding and predicting drug interactions that precipitate serotonin toxicity. J Psychopharmacol 25: 429–436.

Harvey SC (1980). Antiseptics and disinfectants; fungicides, ectoparasiticides. In: Goodman AG, Goodman LS, Gilman A, Mayer SE, Melmon KL (eds). Goodman and Gilman's The Pharmacological Basis of Therapeutics. Macmillan Publishing Company Incorporated: New York, p. 980.

Hilber B, Scholze P, Dorostkar MM, Sandtner W, Holy M, Boehm S et al. (2005). Serotonin-transporter mediated efflux: a pharmacological analysis of amphetamines and non-amphetamines. Neuropharmacology 49: 811–819.

Isbister GK, Buckley NA (2005). The pathophysiology of serotonin toxicity in animals and humans: implications for diagnosis and treatment. Clin Neuropharmacol 28: 205–214.

Kartha SS, Chacko CE, Bumpous JM, Fleming M, Lentsch EJ, Flynn MB (2006). Toxic metabolic encephalopathy after parathyroidectomy with methylene blue localization. Otolaryngol Head Neck Surg 135: 765–768.

Kuriloff DB, Sanborn KV (2004). Rapid intraoperative localization of parathyroid glands utilizing methylene blue infusion. Otolaryngol Head Neck Surg 131: 616–622.

Mayer B, Brunner F, Schmidt K (1993). Inhibition of nitric oxide synthesis by methylene blue. Biochem Pharmacol 45: 367–374.

Miller KJ, Hoffman BJ (1994). Adenosine A3 receptors regulate serotonin transport via nitric oxide and cGMP. J Biol Chem 269: 27351–27356.

Moncada S, Higgs EA (2006). Nitric oxide and the vascular endothelium. Handb Exp Pharmacol 176: 213–254.

Muller T (1992). Light-microscopic demonstration of methylene blue accumulation sites in mouse brain after supravital staining. Acta Anat (Basel) 144: 39–44.

Muslumanoglu M, Terzioglu T, Ozarmagan S, Tezelman S, Guloglu R (1995). Comparison of preoperative imaging techniques (thallium technetium scan and ultrasonography) and intraoperative staining (with methylene blue) in localizing the parathyroid glands. Radiol Med 90: 444–447.

Naylor GJ, Martin B, Hopwood SE, Watson Y (1986). A two-year double-blind crossover trial of the prophylactic effect of methylene blue in manic-depressive psychosis. Biol Psychiatry 21: 915–920.

Naylor GJ, Smith AH, Connelly P (1987). A controlled trial of methylene blue in severe depressive illness. Biol Psychiatry 22: 657–659.

Ng BK, Cameron AJ (2010). The role of methylene blue in serotonin syndrome: a systematic review. Psychosomatics 51: 194–200.

O'Leary JC 3rd, Li Q, Marinec P, Blair LJ, Congdon EE, Johnson AG *et al.* (2010). Phenothiazine-mediated rescue of cognition in tau transgenic mice requires neuroprotection and reduced soluble tau burden. Mol Neurodegener 5: 45.

Oz M, Lorke DE, Petroianu GA (2009). Methylene blue and Alzheimer's disease. Biochem Pharmacol 78: 927–932.

Oz M, Jaligam V, Galadari S, Petroianu G, Shuba YM, Shippenberg TS (2010a). The endogenous cannabinoid, anandamide, inhibits dopamine transporter function by a receptor-independent mechanism. J Neurochem 112: 1454–1464.

Oz M, Libby T, Kivell B, Jaligam V, Ramamoorthy S, Shippenberg TS (2010b). Real-time, spatially resolved analysis of serotonin transporter activity and regulation using the fluorescent substrate, ASP+. J Neurochem 114: 1019–1029.

Oz M, Lorke DE, Hasan M, Petroianu GA (2011). Cellular and molecular actions of methylene blue in the nervous system. Med Res Rev 31: 93–117.

Peter C, Hongwan D, Kupfer A, Lauterburg BH (2000). Pharmacokinetics and organ distribution of intravenous and oral methylene blue. Eur J Clin Pharmacol 56: 247–250.

Ramamoorthy S, Giovanetti E, Qian Y, Blakely RD (1998). Phosphorylation and regulation of antidepressant-sensitive serotonin transporters. J Biol Chem 273: 2458–2466.

Ramsay RR, Dunford C, Gillman PK (2007). Methylene blue and serotonin toxicity: inhibition of monoamine oxidase A (MAO A) confirms a theoretical prediction. Br J Pharmacol 152: 946–951.

Schmid JA, Scholze P, Kudlacek O, Freissmuth M, Singer EA, Sitte HH (2001). Oligomerization of the human serotonin transporter and of the rat GABA transporter 1 visualized by fluorescence resonance energy transfer microscopy in living cells. J Biol Chem 276: 3805–3810.

Schwartz JW, Blakely RD, DeFelice LJ (2003). Binding and transport in norepinephrine transporters. Real-time, spatially resolved analysis in single cells using a fluorescent substrate. J Biol Chem 278: 9768–9777.

Schwartz JW, Piston D, DeFelice LJ (2006). Molecular microfluorometry: converting arbitrary fluorescence units into absolute molecular concentrations to study binding kinetics and stoichiometry in transporters. Handb Exp Pharmacol 175: 23–57.

Volke V, Wegener G, Bourin M, Vasar E (2003). Antidepressant- and anxiolytic-like effects of selective neuronal NOS inhibitor 1-(2-trifluoromethylphenyl)-imidazole in mice. Behav Brain Res 140: 141–147.

Wainwright M, Crossley KB (2002). Methylene Blue–a therapeutic dye for all seasons? J Chemother 14: 431–443.

Walter-Sack I, Rengelshausen J, Oberwittler H, Burhenne J, Mueller O, Meissner P *et al.* (2009). High absolute bioavailability of methylene blue given as an aqueous oral formulation. Eur J Clin Pharmacol 65: 179–189.

Zapata A, Kivell B, Han Y, Javitch JA, Bolan EA, Kuraguntla D *et al.* (2007). Regulation of dopamine transporter function and cell surface expression by D3 dopamine receptors. J Biol Chem 282: 35842–35854.

Zhu CB, Hewlett WA, Feoktistov I, Biaggioni I, Blakely RD (2004). Adenosine receptor, protein kinase G, and p38 mitogen-activated protein kinase-dependent up-regulation of serotonin transporters involves both transporter trafficking and activation. Mol Pharmacol 65: 1462–1474.

Zhu CB, Steiner JA, Munn JL, Daws LC, Hewlett WA, Blakely RD (2007). Rapid stimulation of presynaptic serotonin transport by A(3) adenosine receptors. J Pharmacol Exp Ther 322: 332–340.